Mass Loss from Thin Liquid-Surface Films Exposed to Re-Entry Heating and Shear

JOHN R. SCHUSTER*
McDonnell Douglas Astronautics Company, Huntington Beach, Calif.

A series of experiments were conducted in order to evaluate the effects of simultaneous high surface heating and high shear on mass loss from thin water films. The conditions simulated are typical of those experienced on the conical forebody of a high-ballistic coefficient re-entry vehicle. The test results showed mass loss to be a strong function of surface shear, and for the conditions investigated shear accounted for from 75%–97.5% of the loss. A correlation found in the literature has yielded reasonably good agreement with the test results.

Nomenclature

A = area, ft^2
C_p = specific heat, Btu/lbm-°R
d, e = Eq. (9), exponent, entrainment factor, dimensionless.
g_c = conversion factor, 32.17 lbm-ft/lbf-sec^2
H = enthalpy, Btu/lbm
$\dot{M}$ = liquid flow rate, lbm/sec
N_c = enthalpy heat-transfer coefficient, lbm/ft^2-sec
Pr = Prandtl number, dimensionless
$\dot{q}$ = heat flux, Btu/ft^2-sec
r = Eq. (8), roughness factor, dimensionless
S = running length, ft
T = temperature °R
U = velocity, fps
X_r = Eq. (10), roughness parameter, lbf$^{1/2}$/ft
X_e = Eq. (11), entrainment parameter, lbf$^{-1/2}$
x = length of a liquid film element, ft
μ = viscosity, lbm/ft-sec
ρ = density, lbm/ft^3
σ = surface tension lbf/ft
τ = shear, lbf/ft^2

Subscripts

e = value at edge of boundary layer
ideal = thermally ideal value with mass transfer
in = added to liquid film
k = kth element of liquid film
lost = lost from liquid film
o = value without mass transfer
r = recovery value
rad = radiation

Superscript

$*$ = value based on reference enthalpy

Introduction

TRANSPIRATION cooling has long been considered to be a good thermal protection technique for systems exposed to high-enthalpy, high-surface heating environments. For the past several years, it has been under investigation for re-entry vehicle nose tips. More recently, it has been considered as a back-up leading edge design solution to meet the reuseability requirements imposed on the Space Shuttle.

Liquid coolants are generally considered to be more effective than gases because they offer the additional benefit of latent heat absorption. As excess coolant is usually ejected in order to provide a margin of safety, it is desirable to know the effect that this liquid will have on attenuating the heat flux in regions downstream of the transpiration cooled section. In part of this region, a liquid film should exist, effectively insulating the surface from the external gaseous boundary layer.

Several studies [1–14] have been conducted in the past on liquid film stability and liquid interaction with gaseous boundary layers. However, these studies have been restricted to evaluating the effects of Mach number and Reynolds number and have been mostly concerned with the physical characteristics of the liquid film/boundary-layer interface. In order to provide basic quantitative as well as qualitative design data, an experimental investigation was conducted to evaluate the effects of simulated re-entry conditions on mass loss from thin water films. The boundary-layer parameters chosen for simulation were surface heat flux and surface shear. The conditions were a cold-wall heat flux of 2200 Btu/ft^2-sec and surface shears of 120 and 250 psf.

Experimental Apparatus

Test Facility

The facility used in conducting the liquid film tests was the Wave Superheater at the Cornell Aeronautical Laboratory in Buffalo, N.Y. The Wave Superheater is a hot-gas generator which operates on conventional shock tube principles. Reference 15 contains a detailed description of this facility. Maximum conditions obtainable at the rotor exit are 150 atm. total pressure, 2900 Btu/lb total enthalpy, and 8000°R total temperature.

Test Models

Figure 1 is a pretest photograph of one of the four contoured wedge liquid film models tested during the investigation. Each model was approximately 3.0 in. wide, and using the method of Ref. 16, was contoured to yield a slight favorable pressure gradient of -1 atm/in. in the expanding Wave Superheater jet. A negative pressure gradient was desirable in order to reduce the probability of standing shocks and flow separation occurring on the model test surface. Two basic contours, A and B, were tested, and are shown graphically in Fig. 2. The models were of phenolic refrasil and were mounted in a copper holder with a 0.375-in.-radius, water-cooled leading edge. The first 0.3 in. of the model was flat

Received June 23, 1971; revision received November 15, 1971. The experiments described in this paper constitute part of the RESEP II program and were supported by Air Force Contract F04701-68-C-0288. Appreciation is expressed to W. Brofman and G. Johnson for test planning, and T. Holtz for test supervision. R. Oeding assisted in the data reduction. The tests were performed under the direction of R. Strickler and W. King of the Aerospace corporation.

Index categories: Multiphase Flows; Hydrodynamics; Boundary Layers and Convective Heat Transfer—Turbulent.

* Senior Engineer Scientist, Aerothermodynamics.

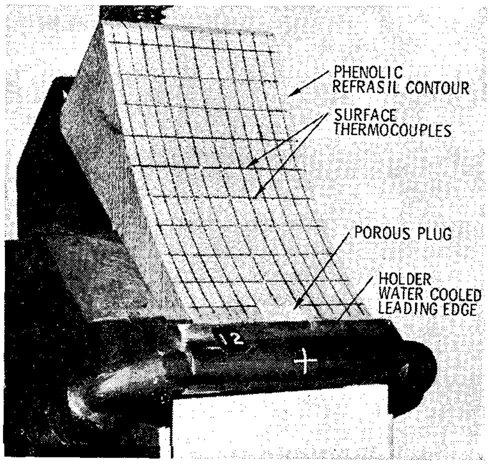

Fig. 1 Pretest liquid film model.

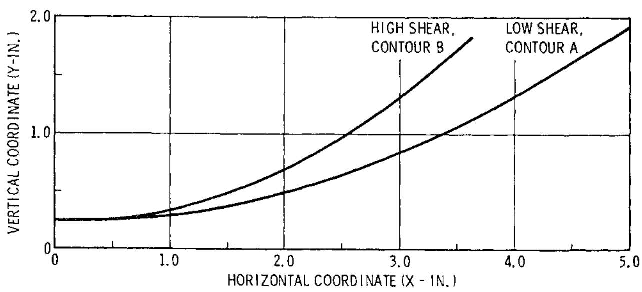

Fig. 2 Model contour profiles.

and during test was inclined approximately 30° to the axis of the jet for contour A and 35° for contour B.

A porous stainless steel plug was located in this flat portion of the models, and provided the flow of water for establishing the liquid films on the model test surface. The exposed surface of the plug was rectangular and measured approximately 0.70 in. by 0.30 in. with the larger dimension cross-wise to the axis of the Wave Superheater jet. The porous plug was set flush with the surface of the model in order to reduce disruption of the boundary layer.

Copper calibration models, duplicating the contours of the liquid film models, were tested in order to measure cold-wall heat flux, and pressure distributions. Heat flux was estimated from transient calorimeters.

The refrasil test surface of the liquid film models was also instrumented with chromel-alumel thermocouples. Model instrumentation was located in patterns that were felt would map the thermal environment in regions covered by liquid films during the test.

Coolant Supply System

The coolant supply system utilized a high-pressure source consisting of five nitrogen bottles pressurized to a maximum of 6000 psi. This pressure was supplied through a 3800 psi relief valve to a 10-quart, chrome-plated, piston-driven, liquid accumulator. The accumulator supplied water to the model through a system of filters and flow measuring equipment.

In addition to flow measurement, expulsion system instrumentation also measured coolant pressure and temperature at a tee fitting used to separate the model instrumentation from the coolant line.

Photographic Equipment

Extensive multicamera, high-speed motion picture coverage was obtained of model surface conditions during the tests; 16 mm photosonics cameras and EFB color film were used.

Test Conditions

The test program included the testing of four liquid film models and three calibration models. The tests were conducted in the freejet of the Wave Superheater in an equilibrium air environment. The conditions that were specified for each test were precalculated to yield desired combinations of heat flux, model surface shear, and pressure gradient. The desired cold-wall heat flux was 2000 Btu/ft^2 sec, the surface pressure gradient -1 atm/in., and the two levels of surface shear were 100 psf and 230 psf. Table 1 summarizes the model locations and actual jet environment during the tests.

Four coolant flow rates were established during each liquid film test. Table 2 presents the actual flow rates and corre-

Table 1 Model locations and environment

CAL run no.	Type test	Duration (sec)	Distance stagnation point to rotor (in.)	Jet total pressure (atm)	Model stagnation pressure (atm)	Jet total temperature (°R)	Jet total enthalpy (Btu/lb)
70-022	Calibration	2.5	2.4	137	37.6	7492	2542
70-023	Liquid film	8.0	2.4	130	35.7	7322	2452
70-041	Calibration	2.5	2.4	145	35.4	7616	2607
70-051	Liquid film	10.0	2.4	137	33.4	7656	2635
70-052	Liquid film	10.0	0.5	121	103	4297	1201
70-053	Liquid film	10.0	2.4	140	34.2	7202	2385
70-062	Calibration	2.5	0.5	122	104	4263	1190

Table 2 Liquid film model coolant flows

CAL run no.	Flow no. 1		Flow no. 2		Flow no. 3		Flow no. 4	
	lb/sec	Time ideal	lb/sec	Time ideal	lb/sec	Time ideal	lb/sec	Time ideal
70-023	0.210	158	0.104	78.2	0.0450	33.8	0.0236	17.8
70-051	0.211	153	0.131	95.0	0.0650	47.0	0.0248	17.9
70-052	0.211	119	0.131	73.6	0.0638	35.8	0.0245	13.8
70-053	0.056	38.6	0.0135	9.31	0.0115	7.94	0.0050	3.45

sponding multiples that they represent of the thermally ideal flow rate. The thermally ideal flow rate was calculated, using the method which is presented later, to be that which was required to cool just the surface of the porous plug assuming that no liquid was entrained in the gaseous boundary layer. The coolant flows varied from 3.45 to 158 times the thermally ideal flow.

Test Results

Figure 3 presents centerline pressure distributions as measured with the calibration models. The low-shear data indicates that the gradient was very close to the planned -1 atm/in. Lateral pressure distributions were also measured and indicated the pressure dropped off from the centerline toward the edges. A variation of approximately 1 atm was observed over the width of the porous plug.

The high-shear centerline gradient was much greater than planned, and averaged approximately -5 atm/in. over the model. Lateral distributions were also greater, although the pressure across the width of the porous plug was nearly constant.

Figure 4 presents the axial, cold-wall, heat-flux distributions obtained with the calibration models. Some of the heat fluxes are off-centerline values. Also shown for comparison is the heat flux calculated using Eq. 1 which is a flat-plate, turbulent, boundary-layer equation based on reference enthalpy.

$$\dot{q}_w = 0.185\,\rho^* U_e Pr^{*-2/3}\,[\log_{10}(U_e S\rho^*/\mu^*)]^{-2.58}\,(H_r - H_w) \tag{1}$$

where the reference enthalpy is evaluated as

$$H^* = 0.28\,H_e + 0.5\,H_w + 0.22\,H_r \tag{2}$$

Boundary-layer edge velocity and enthalpy were computed with an iterative procedure utilizing measured pressures and assuming constant total enthalpy in the flowfield. Running length was measured from the stagnation line on the model holder leading edge. For the low-shear models, flat-plate theory predicts higher than measured heating on the forward portion while providing reasonable agreement on the aft portion. Reasons for the disagreement may include uncertainties in flowfield properties and leading-edge bluntness effects. A heat flux of approximately 2200 Btu/ft^2 sec existed over most of the surface of the low-shear models. The high-shear model centerline heat flux agrees better with prediction, however there is a steep axial gradient. The average heat-flux level over the test surface is approximately the same as that obtained with the low-shear models.

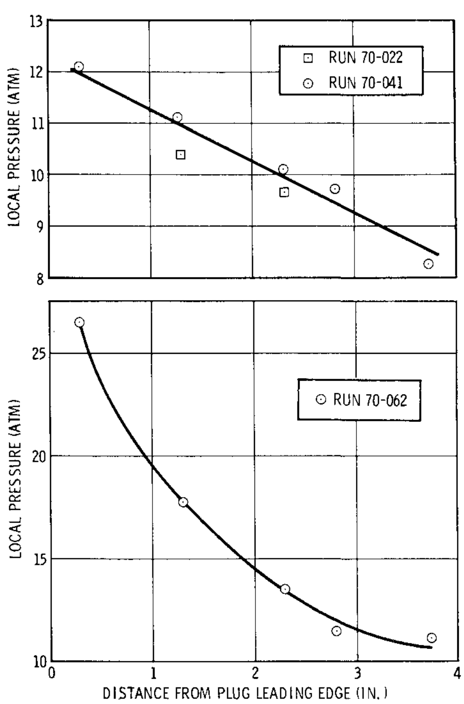

Fig. 3 Centerline pressure distribution.

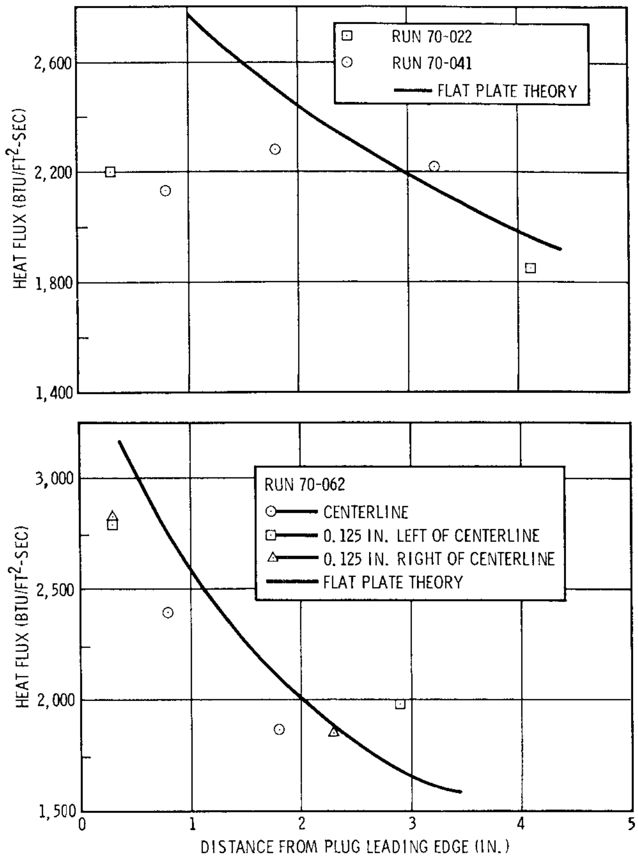

Fig. 4 Axial cold-wall heat-flux distribution.

Utilizing Reynolds analogy in Eq. (3)

$$\tau_w = \dot{q}_w P_r^{*2/3} U_e / g_c (H_r - H_w) \tag{3}$$

the model shear distributions were computed, and are presented in Fig. 5. The shear levels were not constant, but exhibit the same pattern as the heat flux. The levels averaged 120 psf for the low-shear condition and 250 psf for the high-shear condition.

Figure 6 is a post-test photograph of one of the liquid film models. On the phenolic refrasil, an uncharred region exists that was covered by a liquid film for the lowest coolant flow rate during the test. A fairly extensive char region exists downstream, and is interpreted to represent an area in which surface heating was significantly reduced due to the effect of the liquid coolant entrained in the boundary-layer upstream. The areas of greatest surface recession are at the front of the model to the sides of the porous plug, and at the rear of the model towards the centerline. The high recession at the sides of the plug is due to the absence of a liquid film. The calibration data did not indicate excessive heat flux to the rear of the model, nor was a nonuniform pressure distribution measured that might be indicative of shock impingement. It is felt that the unexpected amount of material loss at the rear of the model may be due to water droplet erosion. Figure 7 illustrates the liquid film patterns obtained from the high-speed motion picture coverage of the experiments.

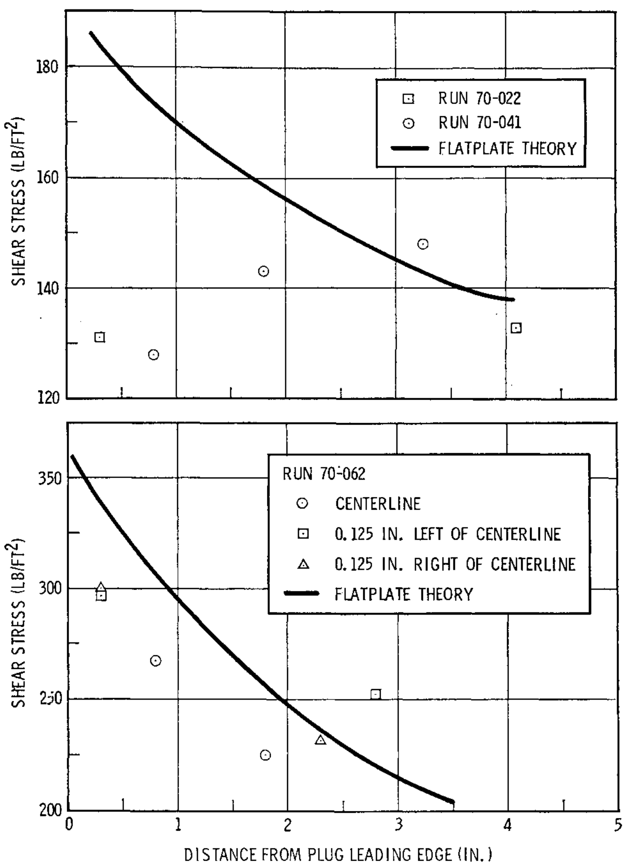

Fig. 5 Axial shear stress distribution.

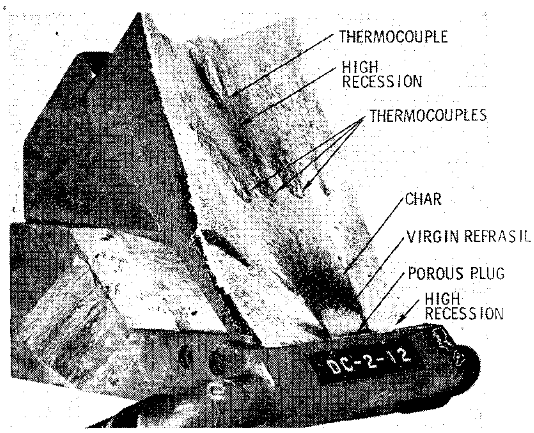

Fig. 6 Post-test liquid film model.

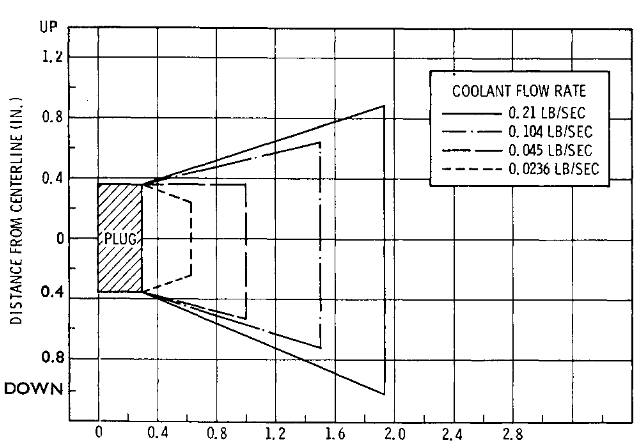

Fig. 7 Average liquid lengths and spreading patterns.

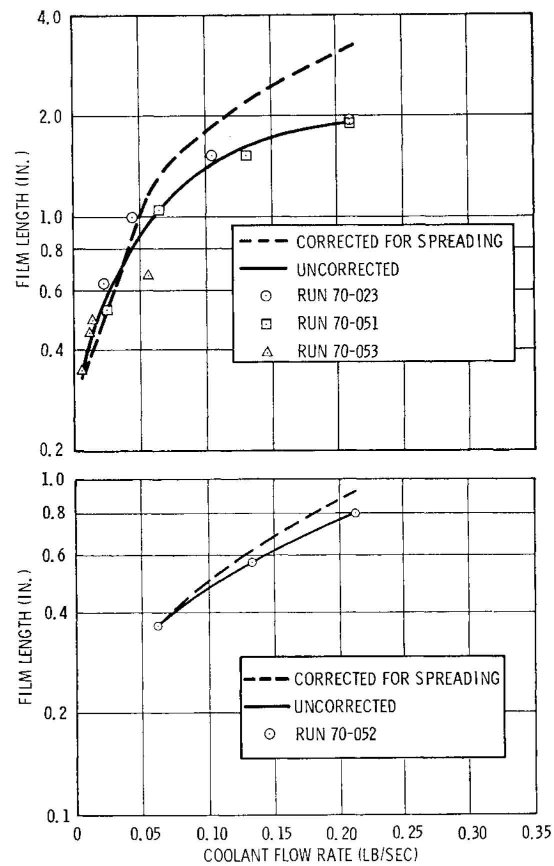

Fig. 8 Liquid film length.

Figure 8 presents the liquid film lengths obtained from the motion pictures. Also shown in this figure is the equivalent film length, correcting for spreading, of a film of constant width equal to the width of the porous plug. The corrected film lengths were greater than the uncorrected except for the lowest flow rates.

Film Length Efficiencies and Gater's Correlation

As an aid in interpreting the liquid film results, it is convenient to express the film lengths as the ratio of actual length (corrected for spreading) to the thermally ideal length that would have occurred if there was no liquid entrainment. This thermally ideal length can be estimated if provision is made for the effect mass transfer in the boundary layer has on altering the surface heat flux from its cold-wall value. This mass transfer blocking effect has been investigated by Bartle and Leadon,[17] Rubesin,[18] Arne,[19] and others.

The traditional form of expressing surface heat flux is that of Eq. (4)

$$\dot{q}_s = (N_c/N_{c0})(\dot{q}_{c0} - \dot{q}_{rad}) \tag{4}$$

where N_c/N_{c0} accounts for the mass transfer effect, and is the ratio of the apparent enthalpy heat-transfer coefficient to the cold-wall, heat-transfer coefficient.

The equation by Arne[19] for a turbulent boundary layer is

$$\frac{N_c}{N_{c0}} = \frac{(C_{P_s}/C_{P_e})^{0.8}\dot{M}_{\text{ideal}}/AN_{c0}}{[1.0 + 0.25(C_{P_s}/C_{P_e})^{0.8}(\dot{M}_{\text{ideal}}/AN_{c0})]^4 - 1.0} \tag{5}$$

where C_{P_s}/C_{P_e} is the ratio of the coolant vapor and freestream specific heats and $\dot{M}_{\text{ideal}}/A$ is the coolant thermally ideal vaporization rate at the surface.

For relatively low-surface temperatures the radiation term in Eq. (4) can be neglected, and utilizing an energy balance

Eq. (4) can be rearranged to yield

$$N_c/N_{c0} = (\dot{M}_{\text{ideal}}/AN_{c0})(\Delta H_c/(H_r - H_s)) \tag{6}$$

where ΔH_c is the enthalpy rise in the coolant, including subcooling and latent heat of vaporization, and the term $(H_r - H_s)$ is the difference between the recovery enthalpy and the free-stream species enthalpy evaluated at the coolant saturation temperature.

Figure 9 presents a graphical solution of Eqs. (5) and (6) for the average conditions existing over the low-shear and high-shear models. Values of 0.52 and 0.69 result for N_c/N_{c0} for the low-shear and high-shear conditions, respectively.

Utilizing these values and the actual coolant flow rates, an energy balance yields the thermally ideal liquid film lengths for each test condition. Gater and L'Ecuyer[20] conducted a series of experiments to evaluate the net rate of mass transfer from thin liquid films to a proximate gas stream. Although their heat flux and shear levels were much lower than those of the present experiments, they developed empirical correlations to account for mass loss due to liquid shearing from the film surface and being entrained into the gaseous boundary layer and also mass loss due to increased heating caused by liquid film surface roughness.

In applying their correlation, the liquid film is divided into a number of equally spaced axial elements. Basing the entrainment rate on the average liquid flow in the element, the mass lost over the surface of the Kth element of unit width and length ΔS is determined from the following equation

$$\dot{M}_{\text{lost},k} = \frac{(1.0 + r_k)\dot{M}_{\text{ideal},k} + e_k\dot{M}_{\text{in},k}}{1.0 + 0.5e_k} \tag{7}$$

where r_k is a film surface roughness parameter

$$r_k = 3.0/X_{r,k}^{0.8} \tag{8}$$

e_k is an entrainment parameter

$$e_k = 1.0 - \exp[-5.0 \times 10^{-5}(X_{e,k} - 1000)(0.833\Delta S)^d] \tag{9}$$

and

$$X_{r,k} = (\rho_e U_e^2/g_c)^{0.5}(T_e/T_s)^{0.25} \tag{10}$$

$$X_{e,k} = X_{r,k}/\sigma \tag{11}$$

In Ref. 20 it is suggested that X_e is analogous to a Webber number. For turbulent boundary layers, it is also suggested that the factor d appearing in Eq. (9) have the value of 0.6.

Figure 10 presents the actual film lengths expressed as a percentage of the thermally ideal length. The solid curves represent a best fit through the data while the dashed curves represent predictions obtained using the correlation of Gater and L'Ecuyer. The low-shear and high-shear data exhibit similar trends. Film length efficiencies are greatest at the lowest flow rate and appear to become asymptotic at high-flow rates. For the conditions investigated, film lengths vary from 6.8%–33% ideal for the low-shear condition and 2.5%–3.5% ideal for the high-shear condition. Also, as flow rate increases, the film length obtained becomes more proportional to shear level.

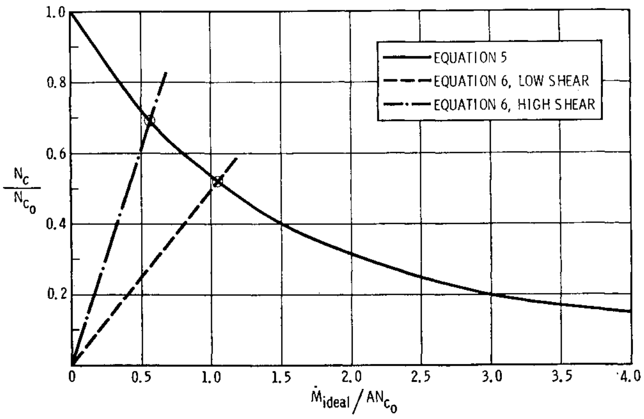

Fig. 9 Heat-transfer coefficient with vaporization.

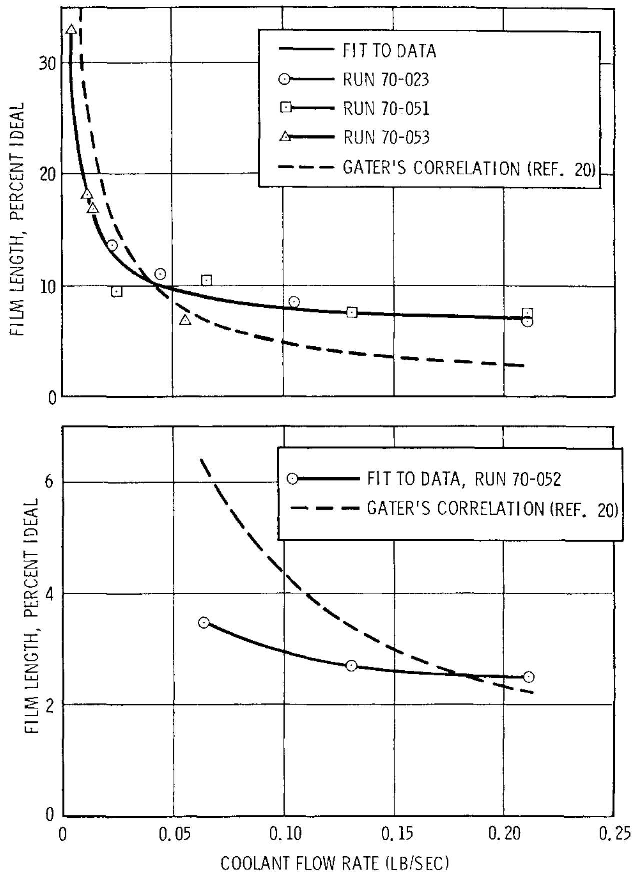

Fig. 10 Film efficiency.

In view of the great difference between the conditions of the present experiments and those of Gater and L'Ecuyer, remarkable agreement is evident. The boundary-layer edge properties used in applying the correlation are those that were obtained in the iterative procedure used to establish the reference enthalpy, flat-plate, heat-flux profiles shown in Fig.4. In view of the disagreement between the measured and estimated heat-flux distributions, these properties, which are used in the correlation of Gater and L'Ecuyer, could be significantly in error.

Conclusions

For the heat-flux and shear conditions investigated, i.e., levels typical of those experienced on the conical forebody of a high-performance re-entry vehicle, shear rather than vaporization appears to be the primary parameter controlling mass loss rate from thin liquid films. The actual film lengths obtained during the experiments vary from 6.8%–33% of the thermally ideal for the low-shear condition, and 2.5%–3.5% ideal for the high-shear condition. Doubling shear, while holding heat flux approximately constant reduces film length efficiencies by between a factor of two and three.

As the thermally ideal film length is increased, due to increasing coolant flow rate, the film length efficiency decreases. This trend is also reflected in the analysis by Gater[20] who deduces that the local liquid entrainment rate is proportional to the flow of coolant within the liquid film. The approach used by Gater shows good promise of correlating high-shear, liquid-film, mass-loss data, and the results of the present experiments might perhaps be used to adjust Gater's correlation to give better agreement for high-shear conditions.

Finally, it appears that liquid entrained in the boundary layer contributes substantially to reducing surface heat flux in a fairly extensive region downstream of where the film terminates. This entrained liquid probably also contributed to the excessive material loss (due to droplet erosion) at the rear of the models.

References

[1] Miles, J., "The Hydrodynamic Stability of a Thin Film of Liquid in Uniform Shearing Motion," *Journal of Fluid Mechanics*, Vol. 8, Aug. 1960, pp. 593–610.

[2] Charvonia, D. A. "A Study of the Mean Thickness of the Liquid-Film and the Characteristics of the Interfacial Surface in Annular, Two-Phase Flow in a Vertical Pipe," Ph.D. thesis, May 1959, Purdue University, Lafayette, Ind.

[3] Lilleleht, L. U. and Hanratty, T. J. "Measurement of Interfacial Structure for Co-current Air-Water Flow," *Journal of Fluid Mechanics*, Vol. 11, 1961, pp. 64–81.

[4] Taylor, N., Hewitt, G. F., and Lacey, P. M. C. "The Motion and Frequency of Large Disturbance Waves in Annular Two-Phase Flow of Air-Water Mixtures," *Chemical Engineering Science*, Vol. 18, Aug., 1963, pp. 537–552.

[5] Wicks, M., and Dukler, A. E. "Entrainment and Pressure Drop in Co-current Gas-Liquid Flow, Part 1," *AIChE Journal*, Vol. 6, Sept., 1960, pp. 463–468.

[6] Craik, A. D. D., "Wind-Generated Waves in Thin Liquid Films," *Journal of Fluid Mechanics*, Vol. 26, Oct., 1966, p. 369.

[7] Cohen, L. S., and Hanratty, T. J. "Generation of Waves in the Concurrent Flow of Air and a Liquid," *AIChE Journal*, Vol. 11, Jan., 1965, pp. 138–144.

[8] Nachtsheim, P. R., "Analysis of the Stability of a Thin Liquid Film Adjacent to a High-Speed Gas Stream," TN D-4976, Jan. 1969, NASA.

[9] Cheng, S. I., and Cordero, J. "Droplet Formation from a Liquid Film over a Rotating Cylinder," *AIAA Journal*, Vol. 1, No. 1, Nov. 1963, pp. 2597–2601.

[10] Gater, R. A., L'Ecuyer, M. R., and Warner, C. F. "Liquid-Film Cooling Its Physical Nature and Theoretical Analysis," Rept. TM-65-6, Oct. 1965, Jet Propulsion Center, Purdue University, Lafayette, Ind.

[11] Hewitt, G. F., and Lacey, P. M. C. "The Breakdown of the Liquid Film in Annular Two-Phase Flow," *International Journal of Heat and Mass Transfer*, Vol. 8, May, 1965, p. 781.

[12] Hartley, D. E., and Murgatroyd, W. "Criteria for the Break-up of Thin Liquid Layers Flowing Isothermally Over Solid Surfaces," *International Journal of Heat and Mass Transfer*, Vol. 7, Sept., 1964, p. 1003.

[13] Cheng, S. I., "Meteoric Ablation Through Interfacial Instability," *ARS Journal*, Vol. 29, Aug., 1959, pp. 579–587.

[14] Feldman, S., "On the Instability Theory of the Melted Surface of an Ablating Body when Entering the Atmosphere," *Journal of Fluid Mechanics*, Vol. 6, July 1959, 11. 131–155.

[15] Fisher, E. B., "Tests of Transpiration Cooled Wedges Conducted in the Wave Superheater Test Facility," CAL AA-2813-Z-3, Feb. 1970, Cornell Aeronautical Lab., Buffalo, N.Y.

[16] Barry, W. T. and Fisher, E. B. "Design and Testing of Ablation Models with Controlled Pressure Gradients," *Proceedings of AIAA/ASME 10th Structures, Structural Dynamics and Materials Conference*, April 1969.

[17] Bartle, E. R. and Leadon, B. M. "The Effectiveness as a Universal Measure of Mass Transfer Cooling for a Turbulent Boundary Layer," *Proceedings of the 1962 Heat Transfer and Fluid Mechanics Institute*, University of Washington, Seattle, Wash., June, 1962, pp. 27–41.

[18] Rubesin, M. W., "An Analytical Estimation of the Effect of Transpiration Cooling on the Heat-Transfer and Skin-Friction Characteristics of a Compressible Turbulent Boundary Layer," TN 3341, Dec. 1954, NACA.

[19] Arne, C. L., "Ablative Materials Subject to Combustion and Thermal Radiation Phenomena," Paper 1851, Jan. 1964, McDonnell Douglas Corp., Santa Monica, Calif.

[20] Gater R. A. and L'Ecuyer, M. R. "A Fundamental Investigation of the Phenomena that Characterize Liquid-Film Cooling," Rept. TM-69-1, Jan. 1969, Jet Propulsion Center, Purdue University, Lafayette, Ind.